

Order-disorder phase-transformation kinetics in *p*-chloronitrobenzene studied by nuclear quadrupole resonance

Carlos A. Meriles, Silvina C. Pérez, Clemar Schurrer, and Aldo H. Brunetti

Facultad de Matemática, Astronomía y Física, Universidad Nacional de Córdoba, Ciudad Universitaria, 5000 Córdoba, Argentina

(Received 8 January 1997; revised manuscript received 13 August 1997)

p-chloronitrobenzene crystallizes in the centrosymmetric space group $P2_1/c$. Since the molecule does not possess an inversion point, the crystal exhibit orientational disorder. Recently, it was found that this compound has an ordered phase stable below 282.6 K. In the present work, we study the order-disorder phase transformation kinetic using nuclear quadrupole resonance. Isothermal transformation curves for nine different temperatures are analyzed following the theory developed by Cahn. In both the order-disorder and disorder-order phase transformation, nucleation seems to take place at grain edges. The nucleation rate νI^E and growth rate γ for different temperatures have been determined. We have systematically observed a time dependence for γ which only remains constant at an early stage of the reaction. This time behavior can be correctly described assuming that the activation energy associated with growth process increases linearly when the nucleus radius reaches a critical value. Experimental data also show that the ordering process is inhibited for temperatures greater than ~ 273 K (far below the phase-transition point at 282.6 K). This behavior seems to be a consequence of the existence of different microscopic environments in the disordered phase. [S0163-1829(97)04445-7]

I. INTRODUCTION

In any crystal possessing a disordered molecular arrangement, the x-ray technique detects the "average molecule" by the superposition of all the molecules located in the same crystallographic position of the average unit cell.¹ A common example of this kind of disorder is the formation of centrosymmetric crystals by molecules without a center of symmetry. This is the case for *p*-chloronitrobenzene (PCNB). This compound crystallizes in the centrosymmetric space group $P2_1/c$ with two molecules per unit cell.² The space lattice has an equal number of points with molecules facing in opposite directions. So, the "average molecule" is in this case obtained by the superposition of two molecules with half-weight atoms.

Recently, it was found that PCNB has a different crystalline phase stable below 282.6 K.³ Although no x-ray structure analysis has been carried out, nuclear quadrupole resonance (NQR),³ and Raman⁴ studies show that this phase is ordered. The present work is concerned with the study of the order \rightleftharpoons disorder phase transformation kinetics using the ³⁵Cl NQR technique. Section II briefly reviews nucleation and growth theory and gives Cahn's expression for isothermal reaction curves for nuclei forming at grain edges. The application of NQR to the study of phase-transformation kinetics and the thermal treatment of the sample are explained in Sec. III. In Sec. IV, we present the measured isothermal transformation curves and propose an explanation for its peculiar time and temperature dependence.

II. THEORY

An order \rightleftharpoons disorder phase transformation goes through the mechanism of nucleation and growth.⁵ The first process is caused by fluctuations due to thermal agitations that bring the atoms/molecules to new positions corresponding to the

product phase. Such an unstable minute region of the new phase within the parent phase is known as an "embryo." When the size of an embryo exceeds a minimum critical size, it is capable of continued existence and is called a "nucleus" of the product phase. The second process requires transfer of atoms/molecules from the material in the interface on to these nuclei of the product phase.

During the formation of nuclei, differences in shapes, sizes, and specific volumes create new surfaces, stresses, and strains. Therefore, nuclei will form only if the net free energy change during their formation is negative. Otherwise, the unstable embryo dissolves into the parent phase.

The nucleation rate, i.e., the number of nuclei that appear per unit volume of the parent phase per unit time, is given by

$$I = k_1 e^{-(\Delta G_c + E_a)/kT}, \quad (1)$$

where ΔG_c is the potential barrier generated by the presence of a surface free energy⁶ and E_a is the activation energy that governs the jump of the atoms/molecules across the interface. k_1 is a constant.

Depending upon the nature of the material and the phase change involved, two types of nucleation may be distinguished, homogeneous and heterogeneous. Homogeneous nucleation takes place when all volume elements of the parent phase are chemically, energetically, and structurally identical. Since all solids contain a variety of defects such as vacancies, impurities, grain boundaries, and so on, perfectly homogeneous nucleation never occurs in practice. Instead, preferred nucleation takes place at defect centers and it is called heterogeneous nucleation. The calculation of the isothermal reaction curves for nuclei forming preferentially at either grain boundaries (where two grains meet) or at edges or corners (three and four grains meeting respectively) is due to Cahn.⁷

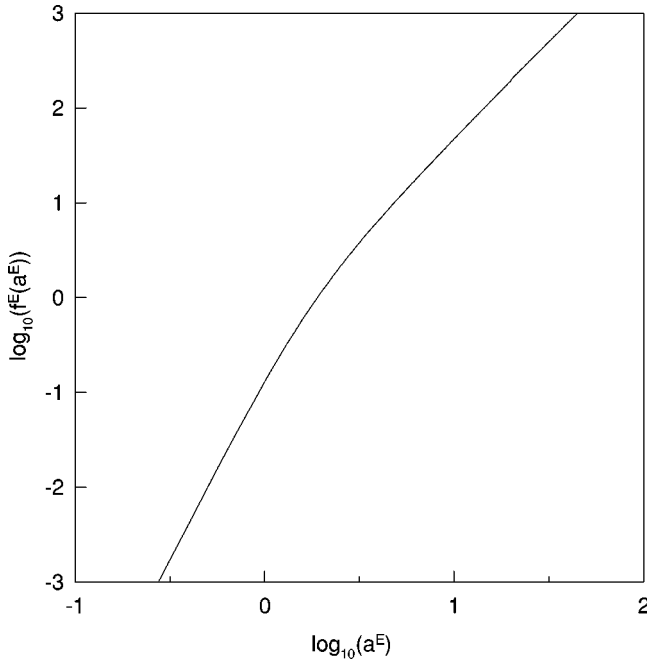


FIG. 1. Master curve for transformations which nucleate on grain edges.

In the particular case that nucleation occurs at edges, the transformed volume fraction at time t is given by

$$\zeta = 1 - \exp\{-(b^E)^{-1}f^E(a^E)\}, \quad (2)$$

where

$$a^E = \left(\frac{vI^E L^2 \gamma}{8.5}\right)^{1/2} t,$$

$$b^E = \frac{vI^E L^4}{2\pi(8.5)^2}$$

$$f^E(a^E) = (a^E)^2 \int_0^1 \xi [1 - \exp\{-(a^E)^2((1 - \xi^2)^{1/2} - \xi^2) \ln\{[1 + (1 - \xi^2)^{1/2}]/\xi\}\}] d\xi.$$

vI^E is the grain edge nucleation rate per unit volume of the assembly, γ is the isotropic growth rate, and L is the mean grain diameter.

When a^E is very small, Eq. (2) approaches the limiting form

$$\zeta = 1 - \exp\{-k_2 \pi^v I^E \gamma^3 t^4\}. \quad (3)$$

When a^E is very large, Eq. (2) has another limiting form:

$$\zeta = 1 - \exp\left\{-\left(\frac{8.5\pi\gamma^2}{L^2}\right)t^2\right\}. \quad (4)$$

The $\{\log_{10}(\ln[1/(1 - \zeta)])\} - \{\log_{10}t\}$ plot thus consists of two straight lines with slopes 4 and 2, separated by an intermediate region over which the slope decreases from 4 to 2. Equation (2) also shows that a $\{\log_{10}f^E(a^E)\} - \{\log_{10}a^E\}$ plot is equivalent to a $\{\log_{10}(\ln[1/(1 - \zeta)]) + \log_{10}b^E\} - \{\log_{10}t + 1/2 \log_{10}(vI^E L^2 \gamma/8.5)\}$ plot. This curve, part of which is shown in Fig. 1, is thus a master curve for all grain

edges nucleated reactions. It is related to an actual $\{\log_{10}(\ln[1/(1 - \zeta)])\} - \{\log_{10}t\}$ plot by two additive constants. Thus, the experimental curve for any reaction to which the theory applies should fit this curve merely by moving the origin.

The change in the slope is known as ‘‘site saturation.’’ It occurs because of saturation of preferential nucleation sites. After saturation, the later stages of the reaction effectively correspond to zero nucleation rate.⁵

Variations of ζ from 0.03 to 0.97 (our maximum observable experimental range) covers only a range of 2.7 in the ordinates of Fig. 1. Therefore it is probable that the whole observable range of reaction will correspond to only a small portion of the curve. Even if the constants are such that site saturation occurs at half transformation, it will be difficult to detect experimentally the change in the slope. Instead, straight lines of intermediate slope will be detected.

When nucleation occurs at grain boundaries or at grain corners, the expressions for ζ are formally equivalent to the expressions presented above. In the first case, the $\{\log_{10}(\ln[1/(1 - \zeta)])\} - \{\log_{10}t\}$ plot takes the limiting form of two straight lines of slopes four and one. When nucleation takes place at grain corners, the straight lines have slopes 4 and 3.

III. EXPERIMENT

Nuclear quadrupole resonance (NQR) is a technique based on the interaction between the nuclear electric quadrupolar moment and the electric field gradient at the nucleus site.⁸ This fact enables to use nuclei as microscopic probes for exploring the electric fields prevailing in solids. In case of first-order phase changes, involving change of crystal structure, the NQR frequency undergoes an abrupt change at the transition temperature. These changes in frequency occur because the electron distribution within the molecules are affected by intermolecular forces, and therefore depend quite sensitively upon the environment around each molecule. In the particular case of disordered systems, the NQR line shape becomes broadened by the static electric field gradient distribution.⁹

It is known that the area under the NQR line shape is proportional to the number of nuclei being observed and its central frequency is typical of the sample’s crystalline phase. Due to the line broadening, the signal amplitude at the central frequency of the disordered phase will be, in our case, about twenty times lower than that observed in the ordered phase. Furthermore, since during the phase transition, no appreciable overlapping between the two lines is present in the measured temperature range (230–283 K), the amplitude related to the ordered phase will not contain any contribution due to the disordered spectrum. In this way, the transformed volume fraction (ζ) will be proportional to the area of this signal. Since, the NQR line width does not change as a function of time, ζ and the NQR amplitude (I), are proportional. Therefore, the time dependence of I in the ordered phase is a good parameter to describe the kinetics of the transformation. This amplitude is obtained from the fast Fourier transform of the second half of the echo signal using a $\pi/2 - \tau - \pi$ pulse sequence with $\tau = 200 \mu\text{s}$.¹⁰

The sample used for these measurements was obtained by spontaneous crystallization of the melt at room temperature and was kept at $T \sim 250$ K for a one year period. Due to the

long time involved, we assumed that the sample was completely ordered. For normalization sake, we measured the NQR signal amplitude as a function of temperature for $T \geq 200$ K. We reached the disordered state by keeping the sample at 284 K for 2 h. Then, we quenched the sample to a lower temperature and, immediately after temperature stabilization, we measured the evolution with time of the NQR signal amplitude. This procedure was repeated for each temperature reported.

The PCNB used for the experiments was obtained from Aldrich Chemical Co. (N C5, 912-2) and used without further purification. The sample container was a cylinder of 1 cm diameter; the amount of sample used was about 2 g. The measurements were taken using a Fourier transform pulse spectrometer.¹¹ The temperature stability was controlled to within 0.1 K using a homemade cryogenic system. Copper-constantan thermocouples were employed for the temperature measurements.

IV. RESULTS AND DISCUSSION

A. Order-disorder transformation kinetics

At 282.6 K the order-disorder transformation process takes place. It is represented in Fig. 2(b). The fact that the disordered phase has a broad line width (~ 300 kHz) and consequently a low amplitude, makes impossible to measure the time evolution of the disordered signal during the transition. Instead, the evolution of the ordered phase signal was measured and the disordered volume fraction has been calculated as

$$\zeta_{\text{dis}} = \frac{V_{\text{dis}}}{V_0} = 1 - \frac{V_{\text{ord}}}{V_0} = 1 - \frac{I_{\text{ord}}}{I_0} \quad (5)$$

where V_0 indicates the sample volume and I_{ord} represents the NQR signal amplitude of the ordered phase. I_0 indicates the NQR amplitude at the very beginning of the phase transition.

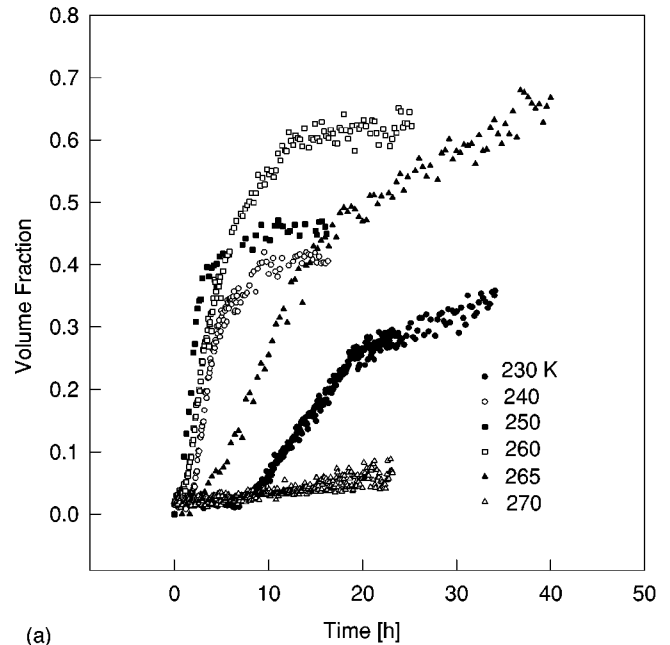
Figure 2(b) is a plot of $\{\log_{10}(\ln[1/(1-\zeta)])\}$ vs $\{\log_{10}t\}$. We observe a linear dependence of slope two. This could be explained assuming grain edge nucleation under the site saturation condition.⁵

B. Disorder-order transformation kinetics

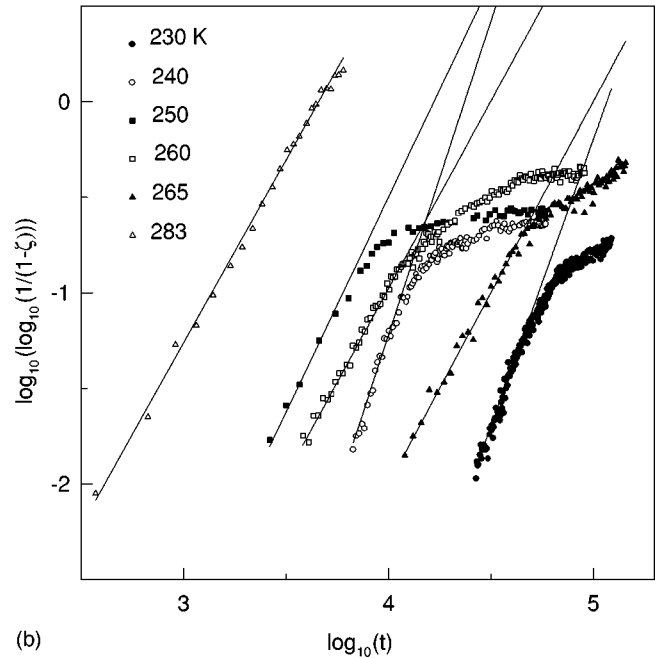
Figure 2(a) shows the time dependence of the transformed fraction for six different temperatures. It is observed that the waiting time necessary to detect the signal has a minimum near 250 K. At the same time, the transformation rate ($d\zeta/dt$) has a maximum close to this temperature. Although the sample does not transform completely in the time observed, the limiting transformed fraction in each case grows with temperature.

Using the scale representation of Fig. 2(b), the time dependence is linear for fractions lower than $\sim 25\%$. Then a change in behavior is observed. After fitting the linear behavior, the slopes of these curves are 3 for 230, 233, 237, and 240 K, 2.7 for 250 K, and 2 for 260 and 265 K. These values of slope are also compatible with grain edge nucleation.

According to the Cahn formalism, the experimental data are related to the master curve by two additive constants which, in turn, can be unambiguously determined only in the



(a)



(b)

FIG. 2. Kinetics of the transformation from the disordered to the ordered phase in PCNB. (a) Transformed volume fraction ζ as a function of t . (b) The master curve for grain edge nucleated reactions is related to these data plot by two additive constants.

case that the data do not show asymptotic behavior (slope 4 or 2). These additive constants allow us to calculate indirectly γ and ${}^v I^E$ from the following expressions:

$$\gamma = \frac{10^{A-B/2}L}{(2\pi 8.5)^{1/2}},$$

$${}^v I^E = \frac{(2\pi)^{1/2}(8.5)^{3/2}10^{A+B/2}}{L^3},$$

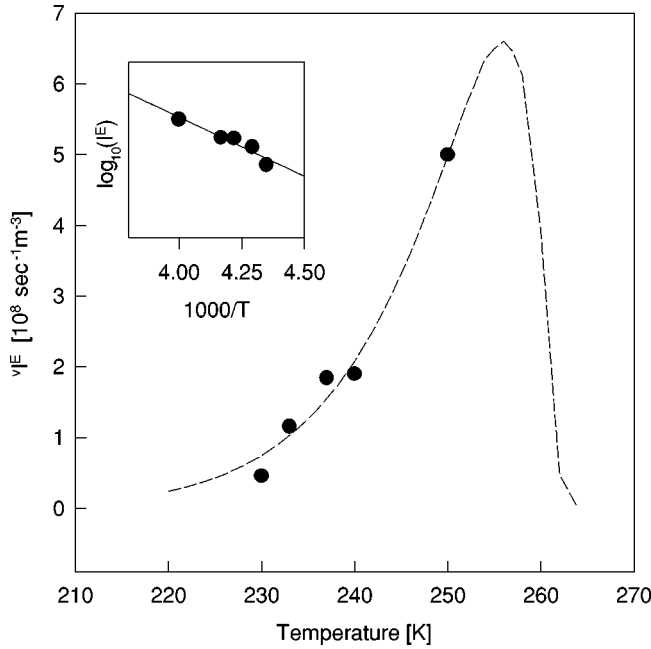


FIG. 3. Plot of nucleation rates as a function of temperature.

where A and B satisfy

$$\log_{10} \left[\ln \left(\frac{1}{1-\zeta} \right) \right] + B = \log_{10} f^E(a^E),$$

$$\log_{10} t + A = \log_{10} a^E.$$

When the slope has the limiting value 2 (after site saturation) it is possible to determine only γ from expression 4. Figures 3 and 4 show the temperature dependence of vI^E and γ calculated assuming a mean grain diameter of 500 μm .

Since we observed a small shift of the NQR central frequency (~ 2 kHz) when the transformed volume fraction is

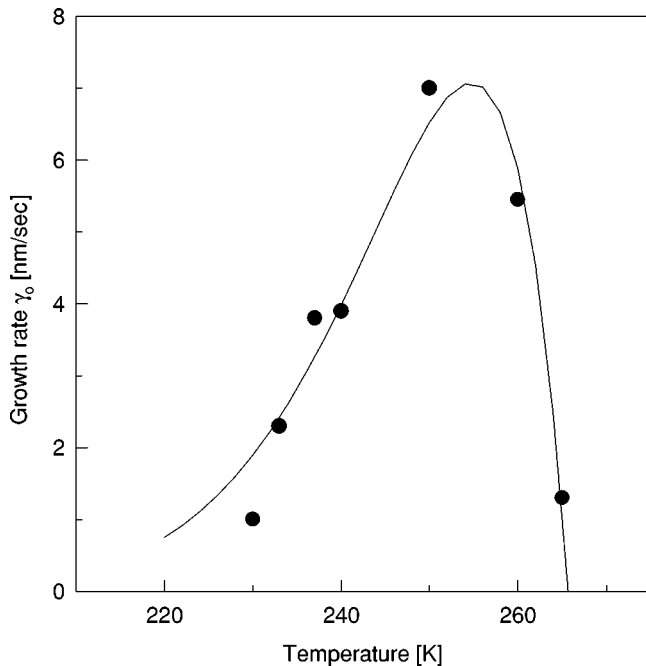


FIG. 4. Plot of growth rates as a function of temperature.

lower than 5%, we assume that the strain energy involved in the nucleation process is low.¹² Then Eq. (1) applies and, as is expected, the behavior of vI^E for $T \leq 250$ K is exponential (see Fig. 3).

If we consider the growth to be achieved through an atom-by-atom transfer across the interface between the two phases, the expected behavior for γ is given by the expression

$$\gamma = k_3 \frac{\Delta H \Delta T}{kT_0} \frac{e^{-E_a/kT}}{T}, \quad (6)$$

where $k_3 \sim 10^3$ m/s is independent of the sample studied.⁶ ΔH is the transformation enthalpy and its value for *p*-Chloronitrobenzene was reported by Meriles *et al.*³ T_0 is the transition temperature.

The solid line shows a least square fit of Eq. (6) to the experimental data with the following parameters:

$$k_3 = 5000 \text{ m/s},$$

$$E_a = 11.7 \text{ K cal/mole},$$

$$T_0 = 265.7 \text{ K}.$$

E_a has a value as expected for a 180° reorientation of an aromatic molecule.^{13,14} This reorientation has necessarily to be present in an ordering process of the crystal. The obtained value for T_0 is lower than the transition temperature determined by differential thermal analysis (DTA).³ This is not surprising since the isothermal transformation curves show that at 270 K the transformation is very slow [see Fig. 2(a)]. This fact can be explained considering the following ideas. In a crystal, the internal energy is given by

$$U = \frac{1}{2} \sum_i \sum_j \varepsilon_{ij},$$

where ε_{ij} is the interaction energy between the i th molecule with the j th molecule. The interaction energy of the i th molecule is $\sum_j \varepsilon_{ij} = \tilde{\varepsilon}_i$. If the crystal is ordered, $\tilde{\varepsilon}_i$ does not depend on i and, disregarding size effects, one obtains

$$U = N \frac{\tilde{\varepsilon}}{2},$$

where N is the number of molecules in the crystal. But if the crystal is disordered

$$U = \sum_i \frac{\tilde{\varepsilon}_i}{2}.$$

In this way, an interaction energy distribution results which, averaged overall the possible configurations, determines the internal energy of the sample. In the present case, this distribution has a width of approximately 3 K cal/mole or more at 0 K.^{1,4}

Since the Gibbs free energy at 0 K equals the internal energy, it is expected that, at higher temperatures, G will be also the average value of a distribution that contemplates the existence of different environments. This distribution will have a finite width probably reduced by thermal agitations. This is schematically represented in Fig. 5. As stated previ-

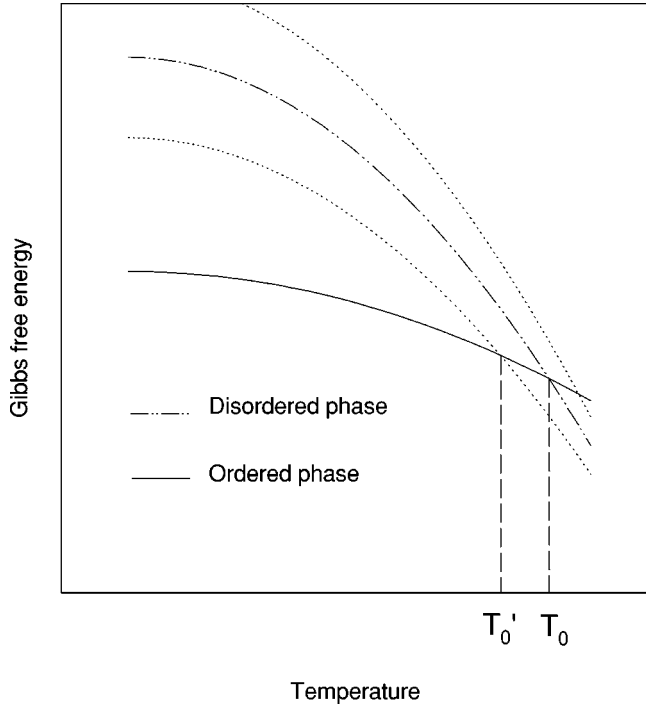


FIG. 5. Schematic representation of the Gibbs free energy as a function of temperature.

ously, in order for the nucleus to form and grow, it is necessary to have a local thermal fluctuation with a negative net free energy. The existence of an energy distribution due to different environments makes possible that some of them will not prematurely satisfy this condition. As a result, an effective T'_0 value lower than the expected one will occur.

Figure 2(b) showed that for volume fractions greater than 25%, the time behavior is not linear. Particularly, at 260 and 265 K, where site saturation is present, one can describe this change in behavior if one considers a time dependence of the growth rate γ . Under sites saturation condition, the growth process along a saturated edge is radial. In this way for a small radius

$$\zeta = \frac{8.5\pi R^2(t)}{L^2}, \quad (7)$$

where

$$R(t) = \gamma_0 t h(t),$$

$$h(t) = \frac{1}{t} \int_0^t g(t') dt',$$

$$g(t') = \gamma(t')/\gamma_0.$$

If impingement is included, then

$$\zeta = 1 - e^{-8.5\pi(R/L)^2} = 1 - e^{-8.5\pi[\gamma_0 t h(t)/L]^2}. \quad (8)$$

The $h(t)$ function can be obtained from the difference $[D(t)]$ between the linear behavior established by Cahn and the experimental data:

$$h(t) = 10^{-D(t)/2}. \quad (9)$$

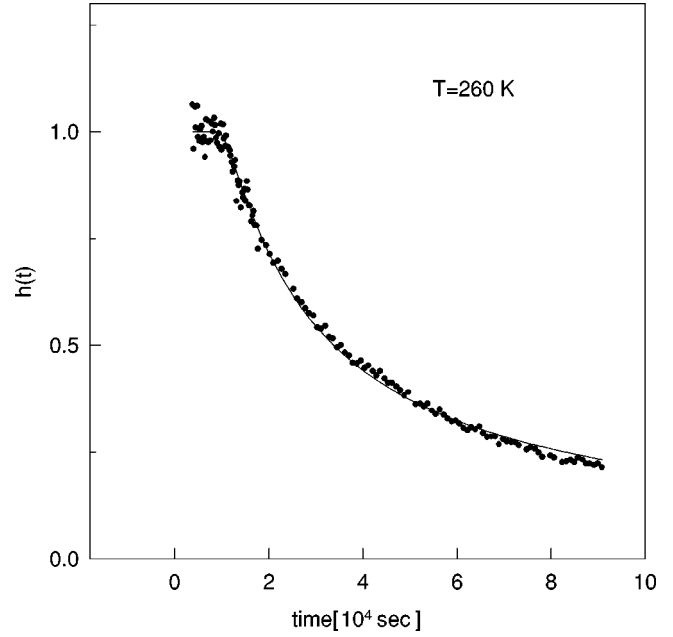


FIG. 6. h as a function of t at $T=260$ K.

This function is shown in Fig. 6 for $T=260$ K. In the range 10^0-10^4 s, $h(t)$ has an average value equal to 1, showing that γ has a constant value equal to γ_0 . For longer times, γ has values progressively smaller than γ_0 . Therefore, $h(t)$ decreases gradually with time. This behavior can be interpreted considering that the activation energy E_a (needed to cross the interface and associated to the molecular reorientation) depends on the radius of the nucleus and therefore on t . In fact, for a crystal with orientational disorder, a distribution of possible environments is present and therefore a distribution of E_a values.¹⁵ If the nucleus grows initially due to favorable environments (minimum E_a), then a progressive segregation of the environments with less favorable energy for the reorientation results. This condition occurs when the nucleus reaches a critical radius $R_0 = \gamma_0 t_0$.

Consequently, the following dependence of $E_a(R)$ and $\gamma(R)$ results:

$$E_a(R) = \begin{cases} E_a, & R \leq R_0, \\ \rho(R - R_0) + E_a, & R \geq R_0, \end{cases} \quad (10)$$

$$\gamma/\gamma_0 = \begin{cases} 1, & R \leq R_0, \\ e^{-\rho(R - R_0)/kT}, & R \geq R_0. \end{cases} \quad (11)$$

Since $\gamma = dR/dt$, one obtains

$$R(t) = R_0 + \frac{kT}{\rho} \ln \left(\frac{\rho \gamma_0}{kT} (t - t_0) + 1 \right), \quad t \geq t_0.$$

Finally

$$h(t) = \begin{cases} 1, & t \leq t_0, \\ \frac{1}{t} \left[t_0 + \frac{kT}{\rho \gamma_0} \ln \left(\frac{kT}{\rho \gamma_0} (t - t_0) + 1 \right) \right], & t \geq t_0. \end{cases} \quad (12)$$

In Fig. 6, the solid line, shows a least squares fit to the experimental data of $h(t)$. The fit yields $t_0 = 8380$ s and $\rho = 13.7$ K/ μm .

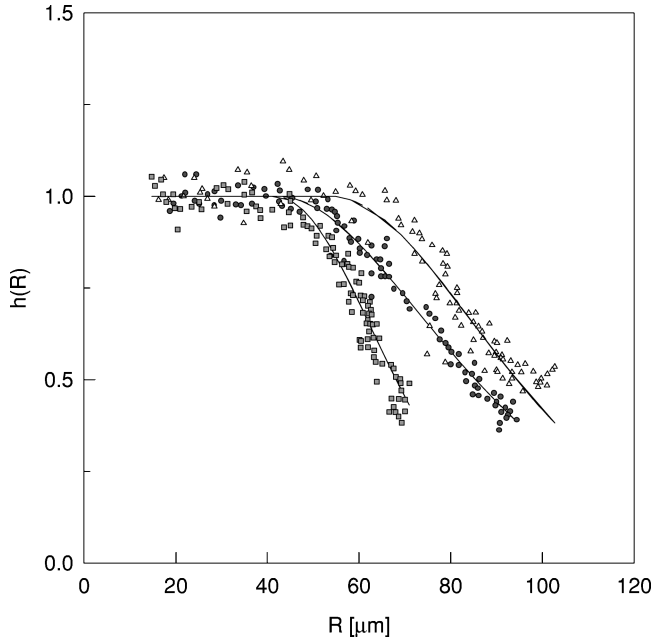


FIG. 7. h as a function of the nucleus radius for three different temperatures.

In order to understand the physical process involved, it is helpful to present the results in terms of R . From Eq. (8), it is possible to calculate an experimental value of R at time t using the expression

$$R[\zeta(t)] = \left[\frac{L^2}{8.5\pi \log_{10} e} \log_{10} \left(\frac{1}{1-\zeta(t)} \right) \right]^{1/2}.$$

Plotting $h(t)$ vs $R(t)$ for each time t , one obtains experimental values for $h(R)$ (Fig. 7). Simultaneously, from the model for $E_a(R)$, it follows that

$$h(R) = \begin{cases} 1, & R \leq R_0, \\ R/R_0 \left[1 + \frac{kT}{\rho\gamma_0} (e^{\rho\Delta R/kT} - 1) \right]^{-1}, & R \geq R_0. \end{cases} \quad (13)$$

The solid line in Fig. 7 shows the least squares fit to experimental data for $h(R)$ for three different temperatures. It is seen that $h(R)$ [and consequently $\gamma(R)$] remains constant until the radius reaches a critical value R_0 , after which a

TABLE I. Temperature dependence of the fitted parameters in Eq. (13).

Temperature	R_0 [μm]	ρ [$\text{K}/\mu\text{m}$]
230	41	24
240	42	21
260	44	12
265	52	13

smooth decrease occurs. The fitted values of R_0 and ρ for all temperatures are summarized in Table I. The R_0 value increases slowly with temperature. On the other hand ρ is a monotonously decreasing function of temperature; this shows that the segregation process due to unfavorable environments is more efficient as the temperature increases.

V. CONCLUSION

Even though the kinetic studies are not concluding respect to the type of nucleation involved, in the order \leftrightarrow disorder phase-transformation process of PCNB the process seems to take place at grain edges. For fractions lower than 25% the growth rate in the disorder-order transformation is constant. Its temperature dependence is the expected one, except that it goes to zero at a lower temperature than that determined by DTA. For fractions higher than 25% it depends on the size of the nucleus. This behavior can be explained if, for a radius greater than a critical one ($R_0 = \gamma_0 t_0$), we assume a linear dependence of the activation energy on the radius.

The ordering process is inhibited for temperatures above 273 K. This behavior could be a consequence of the existence of different microscopic environments in the disordered phase. The volume fraction transformed grows progressively with temperature without transforming completely for the time range observed.

ACKNOWLEDGMENTS

The authors wish to express their thanks to Robin L. Armstrong for helpfully reviewing the manuscript. This research was supported in part by the CONICET of Argentina and in part by the SeCyT-UNC.

¹A. I. Kitaigorodsky, *Molecular Crystals and Molecules* (Academic, New York, 1973).

²T. C. Mak and J. Trotter, *Acta Crystallogr.* **15**, 1078 (1962).

³C. A. Meriles, S. C. Pérez, and A. H. Brunetti, *Phys. Rev. B* **54**, 7090 (1996).

⁴C. A. Meriles, J. Schneider, L. A. de O. Nunes, and A. H. Brunetti (unpublished).

⁵J. W. Christian, *The Theory of Transformations in Metals and Alloys*, 2nd ed. (Pergamon, Oxford, 1975), Pt. 1.

⁶C. N. R. Rao and K. J. Rao, *Phase Transitions in Solids* (McGraw-Hill, New York, 1978).

⁷J. W. Cahn, *Acta Metall.* **4**, 449 (1956).

⁸M. H. Cohen and F. Reif, *Solid State Phys.* **5**, 321 (1957).

⁹T. P. Das and E. L. Hahn, *Solid State Phys.* **1**, 205 (1958).

¹⁰C. P. Slichter, *Principles of Magnetic Resonance* (Springer-Verlag, Berlin, 1980).

¹¹D. J. Pusiol and A. H. Brunetti, *J. Phys. C* **17**, 4487 (1984).

¹²T. Kushida, G. B. Benedek, and N. Bloembergen, *Phys. Rev.* **104**, 5,1364 (1956).

¹³R. K. Boyd, C. A. Fyfe, and D. A. Wright, *J. Phys. Chem. Solids* **35**, 1355 (1974).

¹⁴C. A. Meriles, S. C. Pérez, and A. H. Brunetti, *J. Chem. Phys.* **107**, 1753 (1997).

¹⁵V. G. Karpov and D. W. Oxtoby, *Phys. Rev. B* **54**, 9734 (1996).